

Article

Comparative Extraction of Aluminum Group Metals Using Acetic Acid Derivatives with Three Different-Sized Frameworks for Coordination

Keisuke Ohto ^{1,*}, Nako Fuchiwaki ¹, Hiroaki Furugou ¹, Shintaro Morisada ¹, Hidetaka Kawakita ¹, Marco Wenzel ² and Jan J. Weigand ²

¹ Department of Chemistry and Applied Chemistry, Faculty of Science and Engineering, Saga University, 1-Honjo, Saga 840-8502, Japan; mtp.stc.225@gmail.com (N.F.); sv8227@cc.saga-u.ac.jp (H.F.); morisada@cc.saga-u.ac.jp (S.M.); kawakita@cc.saga-u.ac.jp (H.K.)

² Faculty of Chemistry and Food Chemistry, Technische Universität Dresden, 01062 Dresden, Germany; marco.wenzel@tu-dresden.de (M.W.); jan.weigand@tu-dresden.de (J.J.W.)

* Correspondence: ohtok@cc.saga-u.ac.jp

Abstract: We prepared acetic acid derivatives using three different frameworks, calix[4]arene, alkenyltrimethylol, and trihydroxytriphenylmethane, which differ in the number and size of their coordination sites. We further investigated the extraction properties for aluminum group metal ions. All three extraction reagents exhibited increased extraction compared with the corresponding monomeric compounds, owing to structural effects. The extraction reaction and extraction equilibrium constants were determined using a slope analysis. Their extraction abilities, separation efficiencies, and potential coordination modes are discussed using the extraction equilibrium constants, half-pH values, and spectroscopic data. The calix[4]arene and trihydroxytriphenylmethane derivatives demonstrated allosteric co-extraction of indium ions (In^{3+}) with an unexpected stoichiometry of 1:2.

Keywords: metal separation; host compounds; frameworks; solvent extraction; spectroscopic study; allosteric co-extraction



Citation: Ohto, K.; Fuchiwaki, N.; Furugou, H.; Morisada, S.; Kawakita, H.; Wenzel, M.; Weigand, J.J. Comparative Extraction of Aluminum Group Metals Using Acetic Acid Derivatives with Three Different-Sized Frameworks for Coordination. *Separations* **2021**, *8*, 211. <https://doi.org/10.3390/separations8110211>

Academic Editor: Pavel Nikolaevich Nesterenko

Received: 9 October 2021

Accepted: 3 November 2021

Published: 8 November 2021

Publisher's Note: MDPI stays neutral with regard to jurisdictional claims in published maps and institutional affiliations.



Copyright: © 2021 by the authors. Licensee MDPI, Basel, Switzerland. This article is an open access article distributed under the terms and conditions of the Creative Commons Attribution (CC BY) license (<https://creativecommons.org/licenses/by/4.0/>).

1. Introduction

The seminal discovery of crown ethers by Pedersen in 1967 [1] raised the curtain for “host–guest chemistry” [2]. A series of crown ethers have been synthesized to investigate host–guest complexation with alkali metal ions [3]. Subsequently, various macrocyclic ionophores and frameworks, such as cryptands [4], spherand [5,6], and calixarenes [7], were introduced, and several series of derivatives have been investigated for their alkali metal coordination [8–13]. Most macrocyclic compounds form very stable metal ion complexes, the stability of which depends on how well the cation fits into the cavity formed by the donor atoms [14]. The size-discriminating effect is also the most comprehensible example among the six proposed “structural effects” for host ionophores, like calixarene derivatives [15–17], although there are some more requirements to employ them as extraction reagents [18]. To investigate the size discrimination for a series of homologous metal ions, a well-considered research strategy is required, and the data systematically collected for ionophores of different sizes must be compared in order to contribute to future molecular designs for more effective metal separation.

Our group has synthesized various extraction reagents based on different framework types, namely calix[4]arenes [15,18,19], “trident” molecules as alkenyltrimethylols [16,19–22], and 2,2',2''-trihydroxytriphenylmethane [23]. These frameworks provide unique properties for the synthesis of their derivatives and for metal extraction (Table 1). For the effective separation of metal ions with similar sizes or chemical properties, the synergism of the functional group effect based on the HSAB theory [24] and the above-mentioned structural effect of macrocyclic compounds should be considered [15,18]. Thus,

judicious framework selection is critical for the precise adjustment of the functional groups in order to enable high separation. The employment of assorted frameworks with various properties and different sizes not only contributes to the optimal molecular design of the extraction reagents for a particular separation system, but also expands the range of applications for the separation.

Table 1. Properties of the frameworks.

	Calix[4]arene (Cone)	“Trident” Molecule	Trihydroxytriphenylmethane
Modified group	Active phenols	Non-reactive alcohols	Active phenols
Coordination site (Site size)	small at lower rim (2.0 Å at distal position)	Small and narrow (1.7 Å between O to O)	Small and narrow (less than 2.0 Å)
Inversion (Fixing)	Probable (controllable)	None (already 3-D controlled)	None
Rigidity	Rigid	Relatively rigid	Rigid
Polyfunctionality	e.g., Tetradentate	e.g., Tridentate	e.g., Tridentate
Symmetry	e.g., C ₂ , C ₄ symmetry	e.g., C ₃ symmetry	e.g., C ₃ symmetry
Spectroscopic transparency	UV absorptive	UV Transparent	UV absorptive
Lipophilicity	Poor	Poor	High

Notably, the selection of target metal ions is also important for comparing the effect of different frameworks on the extraction ability and separation efficiency. The trivalent aluminum group metal ions of aluminum, gallium, and indium represent a suitable series of metal ions owing to their congeneric ions. Gallium and indium are employed as raw materials for the fabrication of various advanced materials; however, they do not exist as primary ores and can only be obtained as by-products [25–29]. Their recovery has been summarized in review articles [30,31]. Nishihama et al. reported a systematic extractive separation of Ga³⁺ and In³⁺ by three types of organophosphorus compounds in kerosene with different basicities, their extraction constants in chloride media, and a simulation of their separation by a counter-current mixer-settler cascade with the most suitable extraction reagent (D2EHPA) [32]. New extraction reagents, such as tris(2-hydroxybenzyl)amine [33], aminophosphonic acid [34–36], aminocarboxylic acid [37], phenylphosphinic acid [38], and thioglycolate [39], as well as receptors based on calix[5]arene [40] and calix[4]arene [41,42], have been applied for the separation of Ga³⁺ and In³⁺. Furthermore, we recently investigated Ga³⁺ extraction using secondary amido ligands [43].

In this study, we employed the acetic acid derivatives of three different frameworks, namely a tetraacetic acid derivative of calix[4]arene, a triacetic acid derivative of nonenyltrimethylol, and a triacetic acid derivative of 2,2',2''-trihydroxytriphenylmethane, to investigate the extraction and separation of trivalent aluminum group metal ions. A comparison of the properties of the three frameworks employed to synthesize the extraction reagents is presented in Table 1.

2. Experimental

2.1. Reagents

The chemical structures of the extraction reagents employed in this study are shown in Figure 1. 25,26,27,28-Tetrakis(carboxymethoxy)-5,11,17,23-tetrakis(1,1,3,3-tetramethylbutyl) calix[4]arene (**1**) and the corresponding monomer (**4**) [44], tris(3,5-dimethylpropyl-2-carboxymethoxyphenyl)methane (**3**), and the corresponding monopodal compound (**6**) [23] were synthesized in a manner similar to that reported previously. The purity of compounds (**1**), (**4**), (**3**), and (**6**) was guaranteed by the elementary analysis described in references [44] and [23].

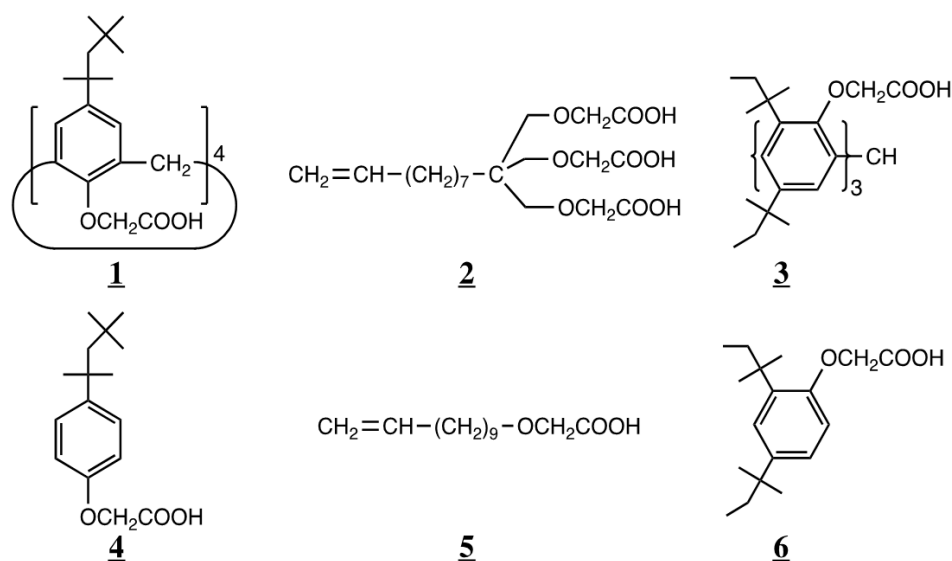
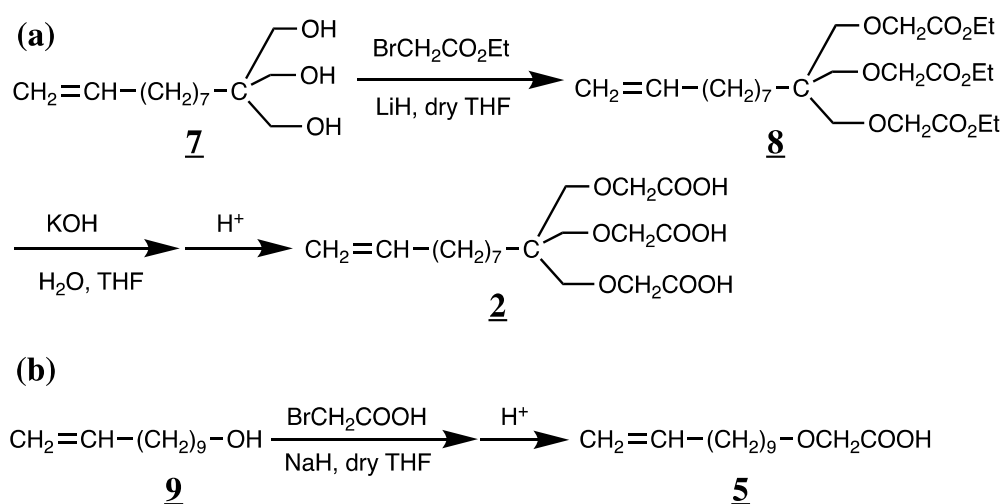


Figure 1. Chemical structures of extraction reagents (1)–(6).

1,1,1-Tris(carboxymethoxymethyl)-9-decene (**2**) was synthesized from 10-undecenal in three steps, as follows: framework preparation [45], followed by esterification and then hydrolysis with a base. The synthetic route to prepare the triacetic acid derivative of nonenyltrimethylol (**2**) is shown in Scheme 1a. The corresponding monopodal compound (**5**) was prepared in a single step from 10-undecen-1-ol, as depicted in Scheme 1b. The obtained compounds were identified by infrared (IR) spectroscopy (Affinity 1, Shimadzu Corporation, Kyoto, Japan) and nuclear magnetic resonance (NMR) spectroscopy (NMR system 400, Varian 400 MHz, Fabreka International, Inc., Stoughton, MA, USA), and the purity was confirmed by thin-layer chromatography (TLC). All other chemicals were purchased and used as received.



Scheme 1. Synthetic scheme of (a) tripodal (**2**) and (b) monopodal (**5**) acetic acid derivatives.

2.1.1.1. 1,1,1-Tris(carboxymethoxymethyl)-9-decene (**2**)

1,1,1-Tris(hydroxymethyl)-9-decene (**7**), was prepared using a previously published procedure [44]. Triol **7** (3.00 g, 13.0 mmol) was added to dry THF (100 cm³) under nitrogen flow. Lithium hydride (0.94 g, 118 mmol, 9.1 eq.) was added, and the mixture was stirred for 30 min at room temperature. Ethyl bromoacetate (13.1 g, 77.9 mmol, 6.0 eq.) was added, and the mixture was heated to 57 °C for 23 h. The reaction was monitored by TLC. After cooling to room temperature, the excess lithium hydride was deactivated with ethanol, and

the solvent was removed under reduced pressure. The desired compound was extracted with chloroform (300 cm³) and washed with 200 cm³ of 1 M HCl (M = mol dm⁻³) and distilled water (300 cm³). The organic solution was dried over anhydrous magnesium sulfate, and the solvent was removed in vacuo to afford 9.36 g of a red-brown viscous liquid as a crude product. A theoretical yield greater than 100% (147%) and the TLC, IR, and ¹H-NMR results indicate the presence of unreacted ethyl bromoacetate, which was used in excess (6.0 eq.). However, in the NMR spectra, only a single resonance at 3.48 ppm was observed, and was assigned to three methylene protons next to the branched carbon atom. Thus, it was assumed that the desired triester, **8**, was formed and the synthesis proceeded without further purification of the intermediate product.

Crude **8** (9.36 g) was dissolved in THF (100 cm³) and distilled water (31.3 g, 1.74 mol), and potassium hydroxide (9.75 g, 173 mmol) was added. The mixture was heated to 63 °C for 23 h and then cooled down to room temperature. The solvent was removed under reduced pressure, and the desired compound was extracted with chloroform (300 cm³) and washed with 100 cm³ of 6 M HCl once and 200 cm³ distilled water twice. The organic solution was dried over anhydrous magnesium sulfate. The solvent was removed in vacuo, and a red-brown viscous liquid was obtained. Yield, 4.68 g (60%); TLC (SiO₂, chloroform:methanol = 9:1, R_f = 0.00–0.37); IR (ATR) disappeared peak ν_{O-H} 3373 cm⁻¹ (br), ν_{O-H} (COOH) 3715–2417 cm⁻¹ (br), ν_{C=O} (COOH) 1728 cm⁻¹, ν_{C-O} 1120 cm⁻¹, ¹H-NMR (400 MHz, CDCl₃, TMS, 30 °C) δ 1.35 (12H, m, 2((CH₂)₆C)), 2.03 (2H, q, CH₂ = CHCH₂), 3.52 (6H, s, C(CH₂)₃), 4.12 (6H, s, (OCH₂COOH)₃), 4.96 (2H, m, CH₂ = CH), 5.80 (1H, m, CH₂ = CH), 8.99 (3H, s(br), (COOH)₃), ¹³C-NMR (100 MHz, CDCl₃, TMS, 30 °C) δ 23–43 ((CH₂)₇C(CH₂)₃), 68 (C(CH₂)₃), 73 (OCH₂COO), 114 (CH₂ = CH), 139 (CH₂ = CH), 175 (COOH). EA for C₁₉H₃₂O₉, calcd C 56.42%, H 7.98%, N 0.00%, found C 56.57%, H 8.04%, N 0.02%. The FT-IR, ¹H-NMR, and ¹³C-NMR spectra of **6** are shown in Figures S1–S3.

2.1.2. 10-Undecenoxyacetic acid (**5**)

10-Undecen-1-ol **9** (1.00 g, 5.89 mmol) was dissolved in dry THF (60 cm³) under a nitrogen atmosphere. The solution was put in a salt ice bath (−12 ± 2 °C) and sodium hydride (0.475 g, 60% in oil, 11.9 mmol, 2.0 eq.) was added. The mixture was stirred for 30 min before bromoacetic acid (3.33 g, 23.9 mmol, 4.1 eq.) was added. The reaction mixture was diluted with 40 cm³ of dry THF and was stirred for 19.5 h at room temperature followed by reflux for 19 h. The reaction progress was monitored by TLC. To enhance the reaction yield, a defined excess of sodium hydride was added to the cooled reaction mixture (ice bath), which was then refluxed for 23 and 21 h, respectively. In the first step, 10 eq. (2.38 g, 60% in oil, 59.6 mmol) sodium hydride was added and in the second step 20 eq. (4.575 g, 60% in oil, 119 mmol) was added. Although the reactant still remained, the mixture was cooled to room temperature, and excess sodium hydride was deactivated with ice water (150 cm³). Diethyl ether (60 cm³) was added to the mixture to extract the desired compounds. The organic phase was washed with 35 cm³ of 6 M HCl and with 30 cm³ of distilled water (three times). The aqueous phase was extracted twice with diethyl ether (60 cm³), and the combined organic solution was dried over anhydrous sodium sulfate. After filtration, the solvent was removed in vacuo and the crude compound was purified by column chromatography (Sfär Silica HC D High Capacity Duo 20 μ 50 g, Isorela prime, Biotage Japan, Tokyo) to obtain a viscous yellow liquid. Yield, 0.223 g (17.7%); TLC (SiO₂, chloroform:2-propanol = 19:1, R_f = 0.00–0.37); IR (neat), ν_{O-H} (COOH) 3500–2450 cm⁻¹ (br), ν_{C-H} 2922 cm⁻¹, ν_{C=O} (COOH) 1732 cm⁻¹, ¹H-NMR (400 MHz, CDCl₃, TMS, 30 °C) δ 1.32 (12H, m, 2((CH₂)₆C)), 1.32 (12H, m, (CH₂CH₂O)), 2.05 (2H, q, CH₂ = CHCH₂), 3.56 (2H, t, CH₂CH₂O), 4.10 (2H, s, OCH₂COOH), 4.96 (2H, m, CH₂ = CH), 5.82 (1H, m, CH₂ = CH), ¹³C-NMR (100 MHz, CDCl₃, TMS, 30 °C) δ 26–34 ((CH₂)₈CH₂O), 68 ((CH₂)₈CH₂O), 72 (OCH₂COOH), 114 (CH₂ = CH), 139 (CH₂ = CH), 174 (COOH). EA for C₁₃H₂₄O₃, calcd C 68.38%, H 10.60%, N 0.00%, found C 69.33%, H 10.76%, N 0.11%. The FT-IR, ¹H-NMR, and ¹³C-NMR spectra of **5** are shown in Figures S4–S6.

2.2. Distribution Study

The extraction study was performed using an experimental procedure described previously [23]. The organic phase was prepared by dissolving the extraction reagent in chloroform to the desired concentration (5 mM for **1–3**, 20 mM for **4**, and 15 mM for **5** and **6**). The aqueous phase was prepared by dissolving each metal nitrate at a concentration of 0.1 mM in 0.1 M HNO₃ or 0.1 M HEPES (N-(2-hydroxyethyl)piperazine-N'-(2-ethanesulfonic acid)). The two aqueous solutions were mixed arbitrarily to adjust the pH values. Equal volumes (2 cm³) of both the organic and aqueous phases were mixed and shaken (150 rpm) for an adequate time at 30 °C. After phase separation, the pH values and metal concentrations were determined using a pH meter (HM-30R, TOA-DKK, Tokyo, Japan) and inductively coupled plasma atomic emission spectrophotometry (ICP-AES, ICPS-8100, Shimadzu Corporation, Kyoto, Japan), respectively. For experiments on the effect of the pH and extraction reagent concentration, pH values between 1.58 and 4.11 and a concentration ranging from 1.0 to 30 mM were used. For comparison of the extraction ability with the carboxylic acid type of commercially available extraction reagent, neodecanoic acid, trade name Versatic acid 10 (**VA10**), was employed and the same procedure was carried out, except for the reagent concentration of 150 mM.

For spectroscopic studies using IR and ¹H-NMR spectra, the metal concentration was adjusted to 12.5 mM. The remaining conditions were the same as those described above, and deuterated chloroform was used. After phase separation, the organic phases containing **4–6** were investigated by IR and ¹H-NMR spectroscopy. The extraction percentage (%E) and distribution ratio (D) were calculated using Equations (1) and (2).

$$\%E = \frac{C_i - C_e}{C_i} \times 100 \quad (1)$$

$$D = \frac{C_i - C_e}{C_e} \quad (2)$$

where C_i and C_e represent the initial and equilibrium metal concentrations in the aqueous phase, respectively.

3. Results and Discussion

3.1. Extraction Rate

The effect of shaking time on the extraction of Al³⁺, Ga³⁺, and In³⁺ was studied using (**1**), (**2**), and (**3**); the results are depicted in Figure 2. The results demonstrate that the extraction equilibrium for all three metal ions in **1–3** was achieved within 12 h, whereas for the more hydrophilic **2**, an overall faster extraction was observed and the equilibrium was reached within 2 h. The relatively slow extraction speed was attributed to the slow horizontal shaking (150 rpm). Furthermore, the rate of the metal extraction of the inner sphere complex, which proceeded through ion exchange and coordination, among other extraction modes, seemed to be related to the Eigen mechanism [46]. The rate of ligand substitution was followed by a weak hydration, in the order of In³⁺ > Ga³⁺ > Al³⁺. Although the same trend was not always followed, the results were generally consistent. The phase separation after shaking was smooth and very immediate without any interruption of the extraction operation.

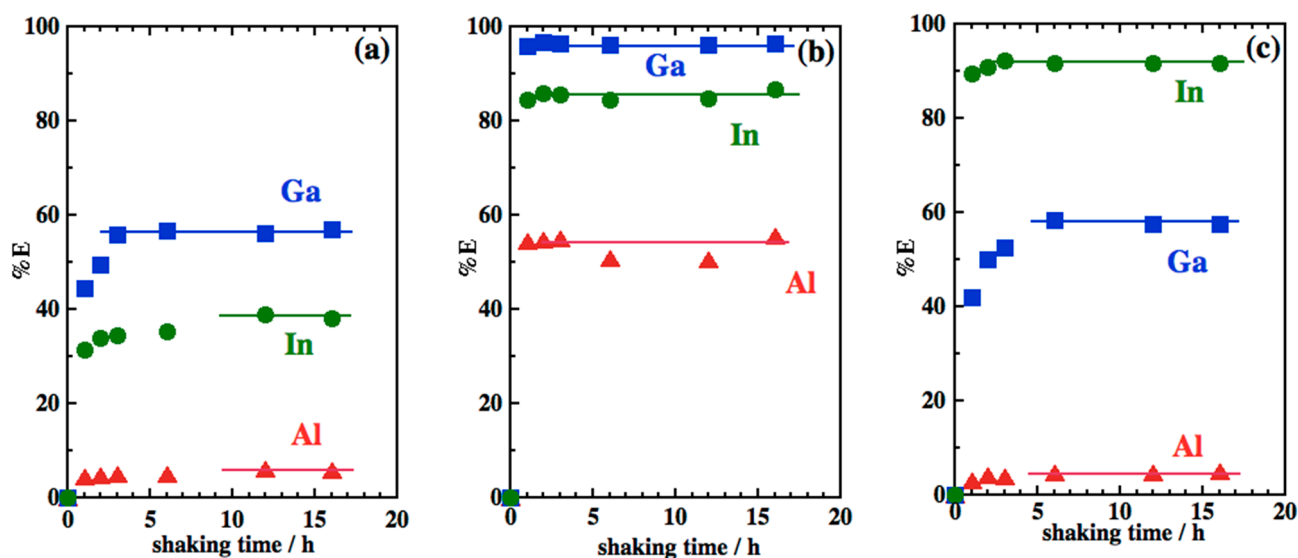


Figure 2. Effect of shaking time on the extraction percentage of Al^{3+} , Ga^{3+} , and In^{3+} with (a) **1**, (b) **2**, and (c) **3**. (a) $\text{pH}_i = 2.90$ for Al and Ga, $\text{pH}_i = 2.40$ for In; (b) $\text{pH}_i = 2.90$; (c) $\text{pH}_i = 2.90$.

3.2. Structural Effect

To evaluate the structural effects, the extraction behavior of the aluminum group metal ions of the calix[4]arene and tripodal extraction reagents **1–3** and the corresponding monomer and monopods **4–6** was studied. The effect of the equilibrium pH on the extraction is illustrated in Figure 3. All extraction reagents contained acetic acid; hence, all acted by a proton/cation exchange mechanism, and the extraction of the three metal ions increased with increasing the pH values. The reagent based on the calix[4]arene and tripodal frameworks **1–3** clearly exhibited a “converging functional group effect” [15–17] and extracted the metal ions at lower pH values than those for their corresponding monomer and monopodal reagents **4–6**. A comparison using extraction equilibrium constants was not possible because of the different extraction reactions for **1–3** and **4–6**. Nevertheless, the reagents based on the calix[4]arene and tripodal frameworks **1–3** were roughly compared with their corresponding monomer and monopodal reagents, **4–6**, using the half pH value, $\text{pH}_{1/2}$, and the difference between the $\text{pH}_{1/2}$ values of two metal ions, $\Delta\text{pH}_{1/2}$. The $\text{pH}_{1/2}$ and $\Delta\text{pH}_{1/2}$ values are listed in Table 2. $\text{pH}_{1/2}$ is the pH value at which 50% of the target ion is extracted (for **2**, the $\text{pH}_{1/2}$ values of all ions were estimated by extrapolating the data with a slope of 3 in Figure 4b.) A lower $\text{pH}_{1/2}$ value represents a high extraction of the reagent and preferable transfer of the metal ion into the organic phase. A larger $\Delta\text{pH}_{1/2}$ value represents the effective separation of the two metal ions. Thus, the $\text{pH}_{1/2}$ is related to the extraction ability and the $\Delta\text{pH}_{1/2}$ value to the separation efficiency. Although all reagents exhibited selectivity in the order of $\text{In}^{3+} > \text{Ga}^{3+} > \text{Al}^{3+}$, detailed discussion can be provided using these values. The $\Delta\text{pH}_{1/2}$ values for three ions between **2** and **5** were much larger than those between **1** and **4** and those between **3** and **6**. The extraction pH ranges of all aluminum group ions with **2** were much lower than those with **1** and **3**, probably due not only to the “converging functional group effect”, but also to the “size discrimination effect” [15–17] or high polarity of the alkenyl trimethylol framework. The $\Delta\text{pH}_{1/2}$ values for the three ions between **3** and **6** were larger than those between **1** and **4**, possibly due to the different coordinating geometries of calix[4]arene derivative **1** and tripodal derivative **3**. The carboxylic acid type of the commercially available extraction reagent, **VA10**, was also employed for obvious evidence of the powerful extraction ability of three reagents, **1–3**. The effect of equilibrium pH on the extraction percentage of Al, Ga, and In with **VA10** is shown in Figure S7. The extraction ability of **VA10** was extremely low owing to the monodentate ligand without any ethereal oxygen atoms for chelation. Although the

concentration of VA10 was adjusted to 150 mM (7.5, 10, and 10 times higher as amount of carboxylic acid groups for **1**, **2**, and **3**), the $pH_{1/2}$ values of In, Ga, and Al were estimated to 3.5, 4.6, and higher than 4.6, respectively.

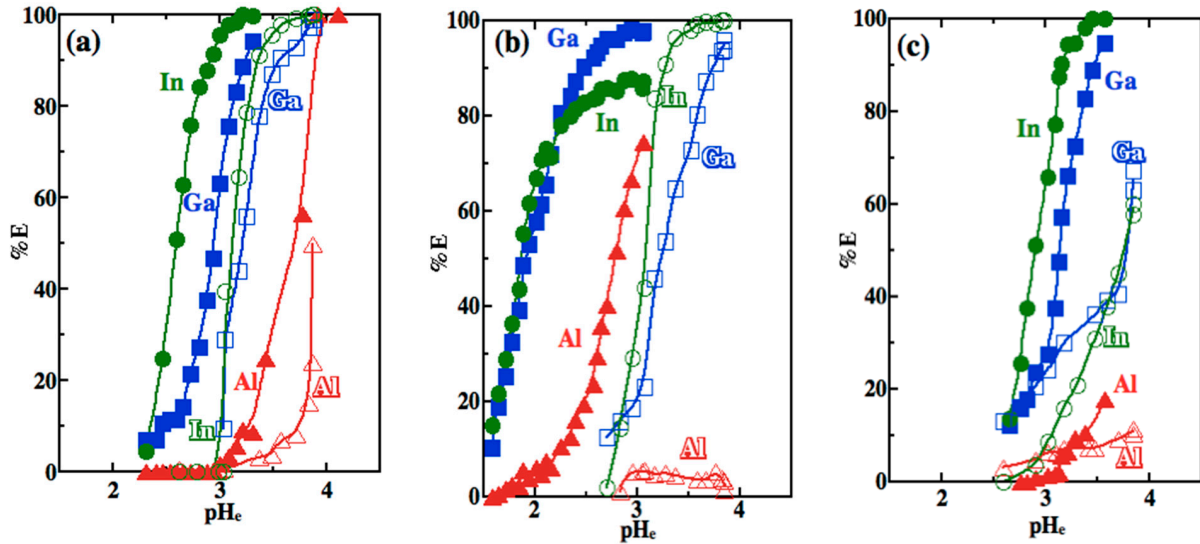


Figure 3. Effect of equilibrium pH on extraction percentage of Al (triangle), Ga (square), and In (circle) with (a) **1** (closed) and **4** (open), (b) **2** (closed) and **5** (open), and (c) **3** (closed) and **6** (open).

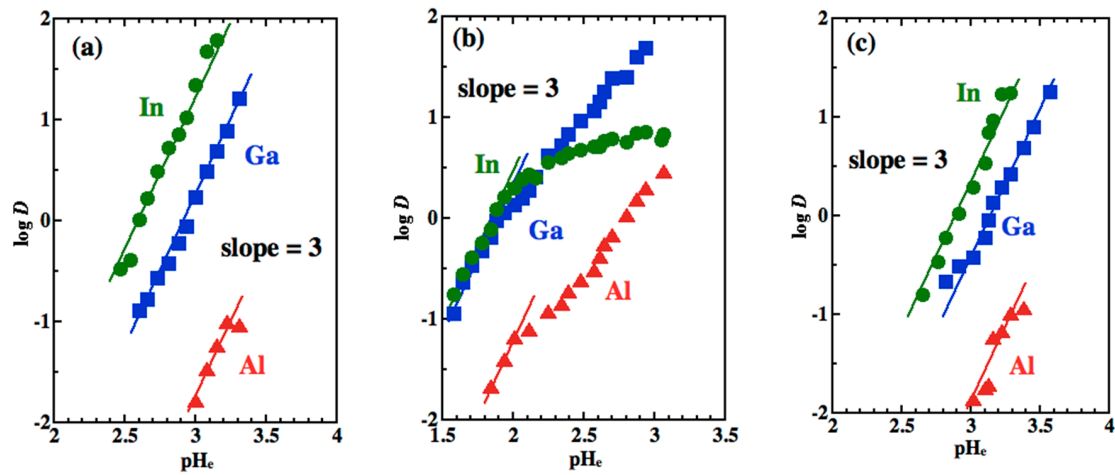


Figure 4. Effect of equilibrium pH on distribution ratio (D) of Al (triangle), Ga (square), and In (circle) with (a) **1**, (b) **2**, and (c) **3**. Extractant= 5 mM. Metal ion = 0.1 mM, 0.1 M HNO_3 –0.1 M HEPES, 30 °C, 150 rpm.

Table 2. Half pH values ($pH_{1/2}$) of aluminum group metal ions with **1**–**6**, and difference in $pH_{1/2}$.

Extractant	Half pH Values, $pH_{1/2}$			$\Delta pH_{1/2}$			$\Delta pH_{1/2}$	
	Al	Ga	In	Al	Ga	In	Al-Ga	Ga-In
1	3.58	2.92	2.60	0.29	0.30	0.52	0.66	0.32
4	3.87	3.22	3.12				0.65	0.10
2	2.41	1.89	1.85	>1.49	1.34	1.23	0.52	0.04
5	>3.90	3.23	3.08				>0.67	0.15
3	3.63	3.14	2.89	>0.22	0.64	0.86	0.49	0.25
6	>3.85	3.78	3.75				>0.07	0.03

The $\Delta\text{pH}_{1/2}$ between Ga^{3+} and In^{3+} with **1** was larger than that with **4**, which indicates that the separation efficiency of **1** was higher than that of **4**, which may be a result of its coordination site being a better fit for In^{3+} . In contrast, the $\Delta\text{pH}_{1/2}$ value between Ga^{3+} and In^{3+} for **2** was smaller than that for **5**, indicating a reduced separation efficiency for **2**. This observation may be as a result of a “negative structural effect” [16,47], and indicates that the coordination site of **2** provides a better fit for Ga^{3+} , or rather is sized somewhere between the ideal sizes for Ga^{3+} and In^{3+} . The $\Delta\text{pH}_{1/2}$ between Ga^{3+} and In^{3+} for **3** was larger than that for **6**, representing a higher separation efficiency of **3**. Presumably, the coordination site of **3** provided a suitable fit for In^{3+} . Furthermore, the $\Delta\text{pH}_{1/2}$ value between Ga^{3+} and In^{3+} for **1** ($\Delta\text{pH}_{1/2,\text{Ga}-\text{In}} = 0.32$) was larger than that for **3** ($\Delta\text{pH}_{1/2,\text{Ga}-\text{In}} = 0.25$), which indicates that In^{3+} fitted better in the coordination site of **1** than that of **3**, and thus, that the coordination site of **1** was larger than that of **3**. Because of the low and unstable extraction with **4–6**, these ligands were no longer considered in the present study.

3.3. Slope Analysis and Extraction Reactions

The stoichiometry for the extraction reaction between the three ions and **1–3** was determined, and the influence of the equilibrium pH on the distribution ratio D is depicted in Figure 4. Most of the determined data points in the $\log D - \text{pH}_e$ diagram lie on the straight lines with a slope of three, which corresponds to the charge of the aluminum group metal ions. Thus, the results strongly suggest that the extraction reactions of all ions are driven by an ion-exchange mechanism with the release of three protons from three carboxyl groups. Note that slopes smaller than three were obtained for **2** for pH values higher than 2 (Figure 4b). Reagent **2** possesses three acetic acid groups and can undergo ion exchange with trivalent ions. Nonenyltrimethylol compounds have a single lipophilic group; consequently, they easily leaked into the aqueous phase, particularly above their pK_a values when three cation-exchangeable groups were introduced. Although the pK_a values of **2** were not determined in this study, the amino derivative of nonenyltrimethylol leaked in the low-pH region [16,21]. Significant changes in the slope for In^{3+} may be caused by the powerful extraction ability of **2** and a mismatch between the coordination size of **2** and that of In^{3+} . The latter may cause incomplete dehydration of In^{3+} .

The dependency of the distribution ratios of the three metal ions on the extractant concentration of **1–3** in the organic phase is illustrated in Figure 5. The plots obtained for the extraction of the three ions with reagents **1–3** were linear with slopes of one, which indicated that each of the three aluminum group metal ions complexed with the reagents at a 1:1 ratio.

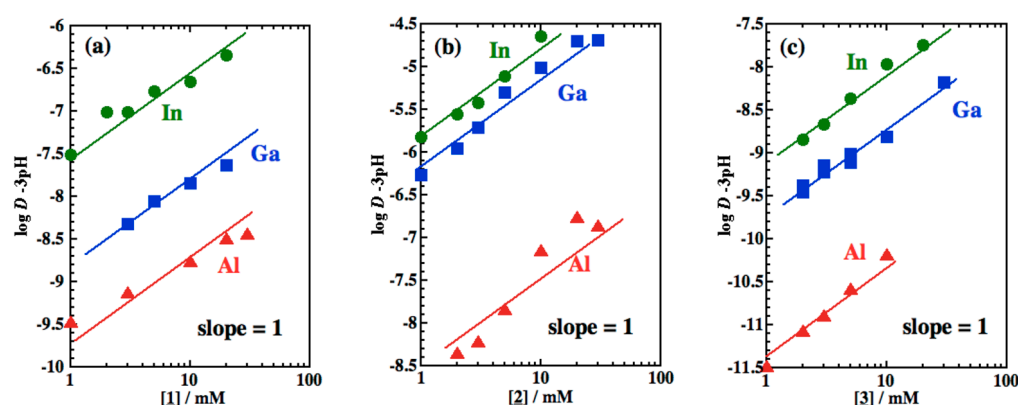
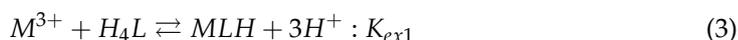


Figure 5. Effect of the extraction reagent concentration on distribution ratio of Al (triangle), Ga (square), and In (circle) with (a) **1**, (b) **2**, and (c) **3**. (a) $\text{pH}_i = 2.84$ for Al, 2.80 for Ga, and 2.45 for In; (b) $\text{pH}_i = 2.75$ for Al, 1.80 for Ga, and 1.77 for In; (c) $\text{pH}_i = 3.70$ for Al, 2.98 for Ga, and 2.70 for In. Metal ion = 0.1 mM; extractant = 1–30 mM; 0.1 M HNO_3 –0.1 M HEPES, 30 °C, 150 rpm.

From the above results, the extraction equation for the aluminum group metal ions with **1** is expressed by Equation (3)



where H_4L represents the calix[4]arene derivative **1**, and K_{ex1} is the extraction equilibrium constant for the trivalent aluminum group metal ions with **1**. The extraction equilibrium constant is expressed by Equation (4).

$$K_{ex1} = \frac{[MLH][H^+]^3}{[M^{3+}][H_4L]} = D \frac{[H^+]^3}{[H_4L]} \quad (4)$$

The distribution ratio (D) is the metal concentration ratio in the organic and aqueous phases, and is defined by Equation (5).

$$D = \frac{[MLH]}{[M^{3+}]} \quad (5)$$

From Equation (4), the relationship between D , pH, and the concentration of **1** is given by Equation (6):

$$\log D = 3pH + \log[H_4L] + \log K_{ex1} \quad (6)$$

The results for the aluminum group metal ions extracted with **1** satisfy Equation (6), and this relationship is represented by a straight line with slopes of three (Figure 4a) and one (Figure 5a) under different conditions.

Similarly, the extraction equation for the aluminum group metal ions with **2** or **3** is expressed by Equation (7).



where H_3L represents either tripodal extraction reagent **2** or **3**, and K_{ex2} is the extraction equilibrium constant for the aluminum group metal ions with **2** or **3**. The extraction equilibrium constant is given by Equation (8). The distribution ratio (D) is defined by Equation (9), and the relationship between D , pH, and the concentration of **2** or **3** is given by Equation (10):

$$K_{ex2} = \frac{[ML][H^+]^3}{[M^{3+}][H_3L]} = D \frac{[H^+]^3}{[H_3L]} \quad (8)$$

$$D = \frac{[ML]}{[M^{3+}]} \quad (9)$$

$$\log D = 3pH + \log[H_3L] + \log K_{ex1} \quad (10)$$

The results obtained for the aluminum group metal ions extracted with **2** or **3** satisfy Equation (10), and show straight lines with a slope of three in the conditions represented in Figure 4b,c, and with a slope of one for the conditions represented in Figure 5b,c. The extraction equilibrium constants of all ions with **1–3**, K_{ex1} and K_{ex2} , and separation factors, $\beta_{Ga/Al}$ and $\beta_{In/Ga}$, were estimated using Equations (6) and (10), together with Equation (11), and are listed in Table 3. With reagent **2**, extraction did not proceed precisely according to Equation (7); however, the extraction equilibrium constants of all ions were estimated using the data with a slope of three, similar to how the $pH_{1/2}$ values were estimated in Figure 4b. With **1** and **3**, the $pH_{1/2}$ and K_{ex} values were also confirmed using Equations (6) and (10), and Figure 4 shows plots with theoretical lines fitted.

$$\beta_{\frac{N}{M}} = \frac{D_{heavier\ ion}}{D_{lighter\ ion}} = \frac{K_{ex, heavier\ ion}}{K_{ex, lighter\ ion}} \quad (11)$$

Table 3. Extraction equilibrium constants of the aluminum group metal ions with **1–3**, and separation factors.

Extractant	Extraction Equilibrium Constants, K_{ex1} and K_{ex2}			Separation Factors, β	
	Al	Ga	In	Ga/Al	In/Ga
1	3.64×10^{-9}	3.48×10^{-7}	3.17×10^{-6}	95.6	9.11
2	1.18×10^{-5}	4.28×10^{-4}	5.64×10^{-4}	36.3	1.32
3	2.58×10^{-9}	7.60×10^{-8}	4.28×10^{-7}	29.5	5.63

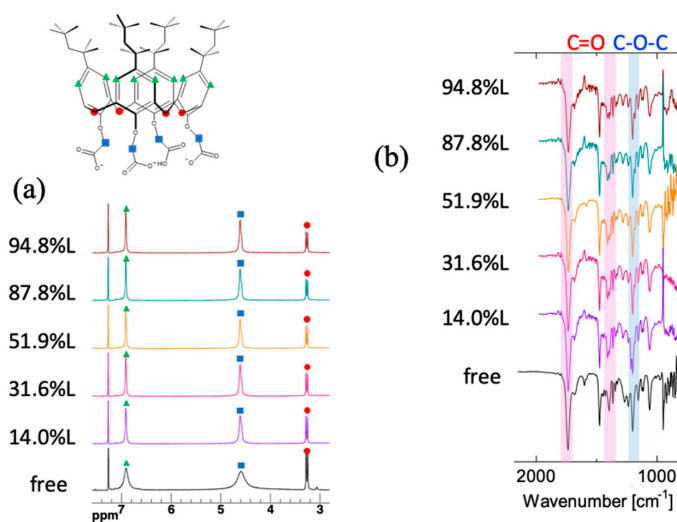
Reagents **1–3** exhibited the same reagent/metal ion stoichiometry (1:1), which allowed for their K_{ex} values to be compared directly. As described above, all reagents exhibited selectivity in the order of $\text{In}^{3+} > \text{Ga}^{3+} > \text{Al}^{3+}$, while **2** exhibited the highest extraction among the ligands with specific structures. Reagent **1**, based on the calix[4]arene framework, exhibited the highest efficiency. As mentioned in the previous section, the $\Delta\text{pH}_{1/2}$ value indicates that the coordination site of **1** is a good fit for In^{3+} . A comparison of the separation factors of **1** and **2** and those of **1** and **3** suggests that the coordination site of **1** may be slightly larger than that of In^{3+} . As explained, the coordination site of **2** is a good fit for Ga^{3+} , or rather, is sized somewhere between the ideal sizes for Ga^{3+} and In^{3+} , while being closer to the size of Ga^{3+} . The coordination site of **3** is a suitable size for In^{3+} , although it is larger than necessary. Further investigations will be carried out in the near future.

3.4. Spectroscopic Studies on the Ga^{3+} - and In^{3+} -Loaded Reagents

$^1\text{H-NMR}$ and IR spectroscopic studies were performed to elucidate the donor atoms of the reagents involved in the metal coordination and to shed light on the relationship between the size of the coordination site and Ga^{3+} and In^{3+} . The $^1\text{H-NMR}$ and IR spectra of the free reagents **1–3**, and those after loading with defined increments of Ga^{3+} and In^{3+} are shown in Figures 6–11. The loading percentages were validated by determining the metal ion concentrations in the aqueous phase before and after loading using ICP-AES measurements. The loading percentage, %L is defined by Equation (12).

$$\%L = \frac{[\text{extracted metal ion}]}{[\text{extraction reagent}]_i} \times 100 \quad (12)$$

where $[\text{extraction reagent}]_i$ represents the initial concentration of the extraction reagent.

**Figure 6.** (a) $^1\text{H-NMR}$ and (b) IR spectra of free **1** and after loading with defined quantities of Ga^{3+} .

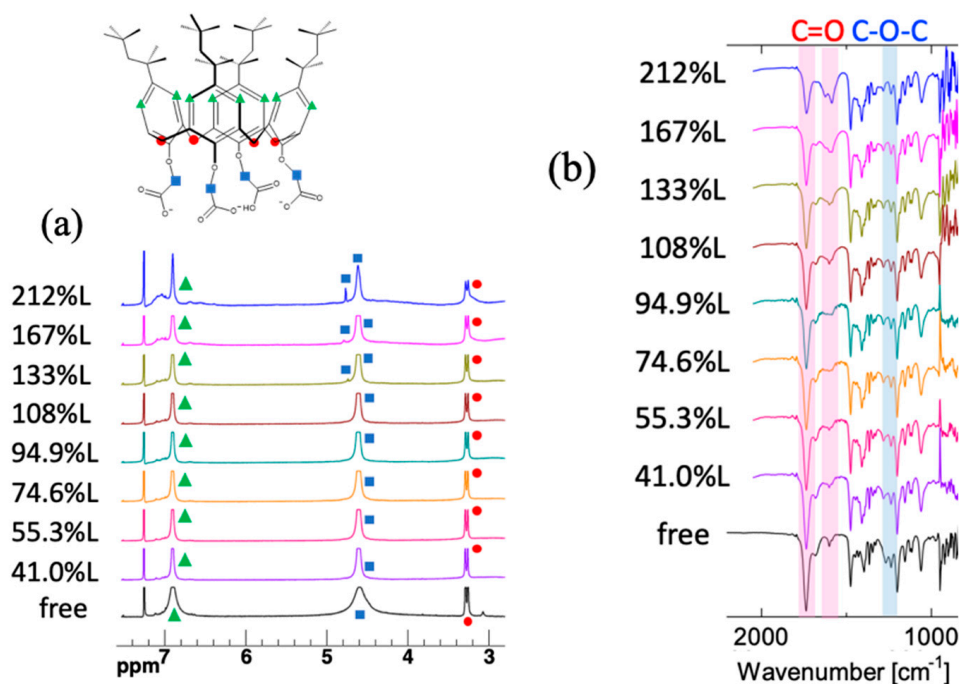


Figure 7. (a) ¹H-NMR and (b) IR spectra of free **1** and after loading with defined quantities of In³⁺.

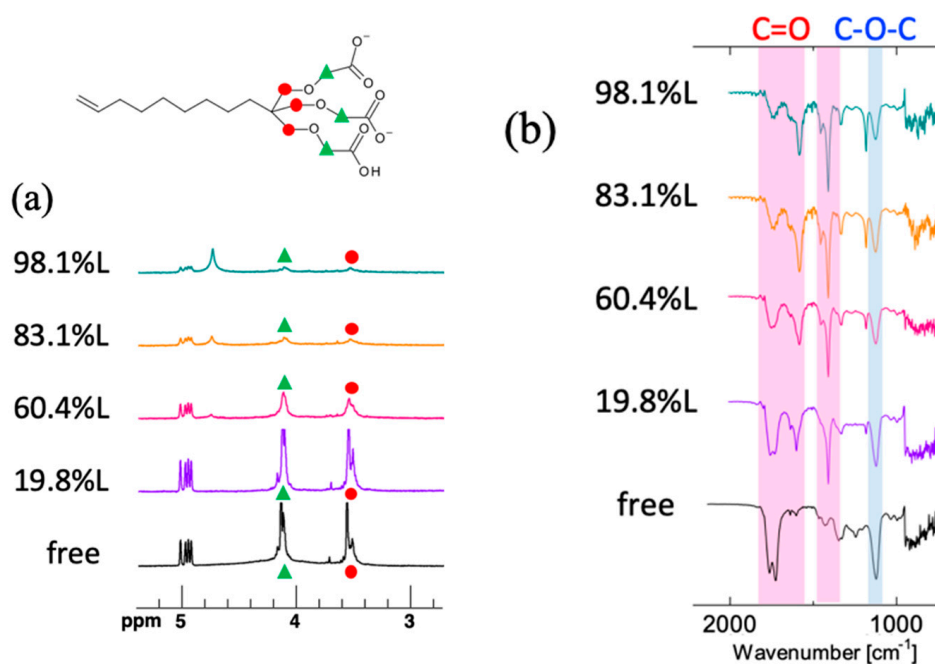


Figure 8. (a) ¹H-NMR and (b) IR spectra of free **2** and after loading with defined quantities of Ga³⁺.

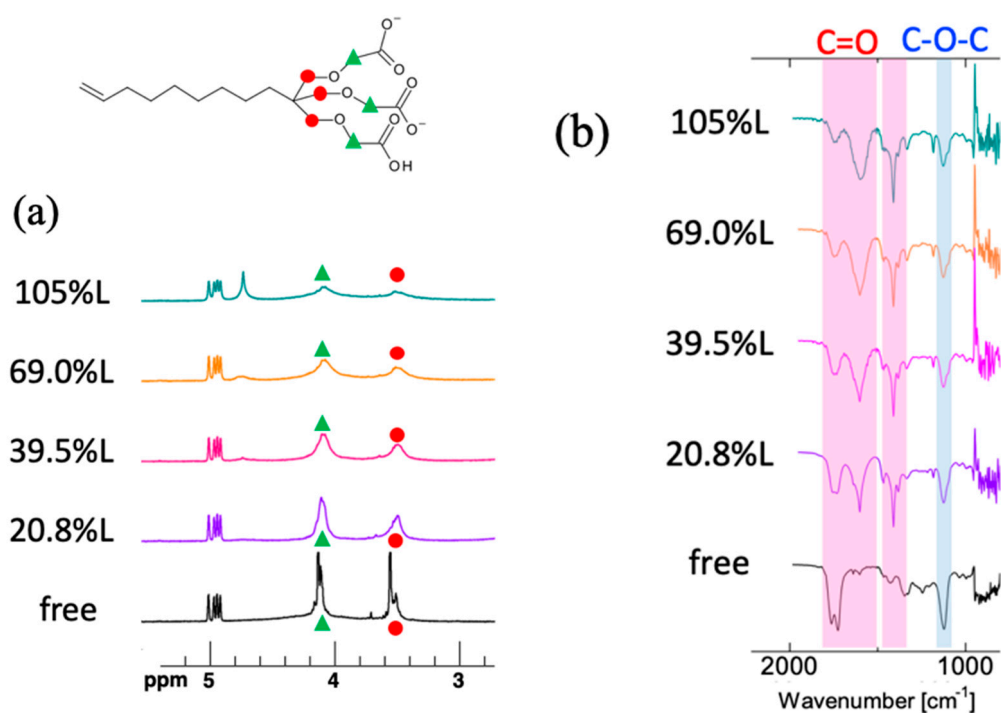


Figure 9. (a) ¹H-NMR and (b) IR spectra of free **2** and after loading with defined quantities of In³⁺.

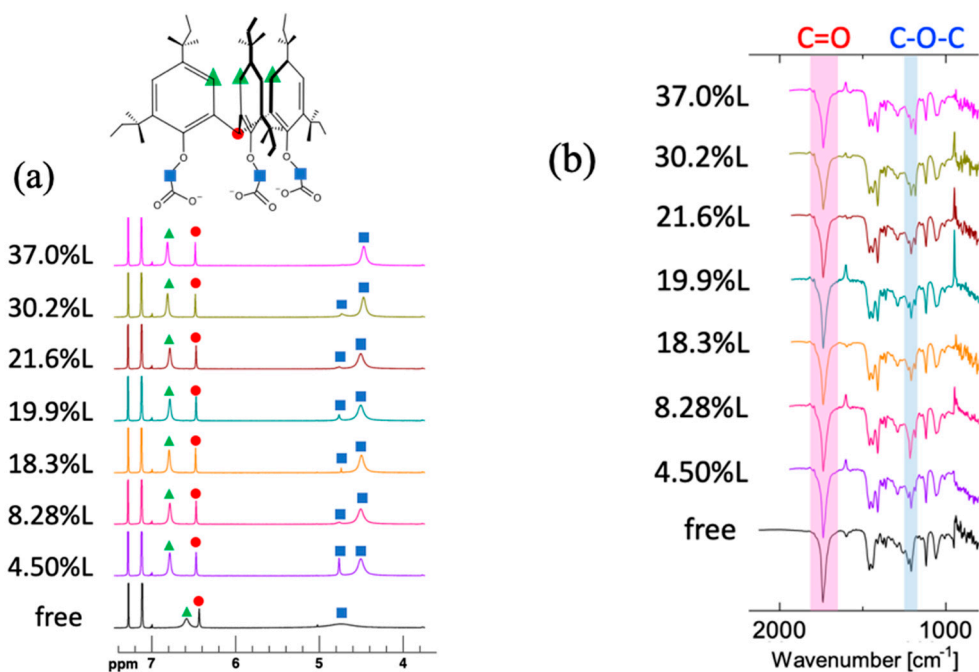


Figure 10. (a) ¹H-NMR and (b) IR spectra of free **3** and after loading with defined quantities of Ga³⁺.

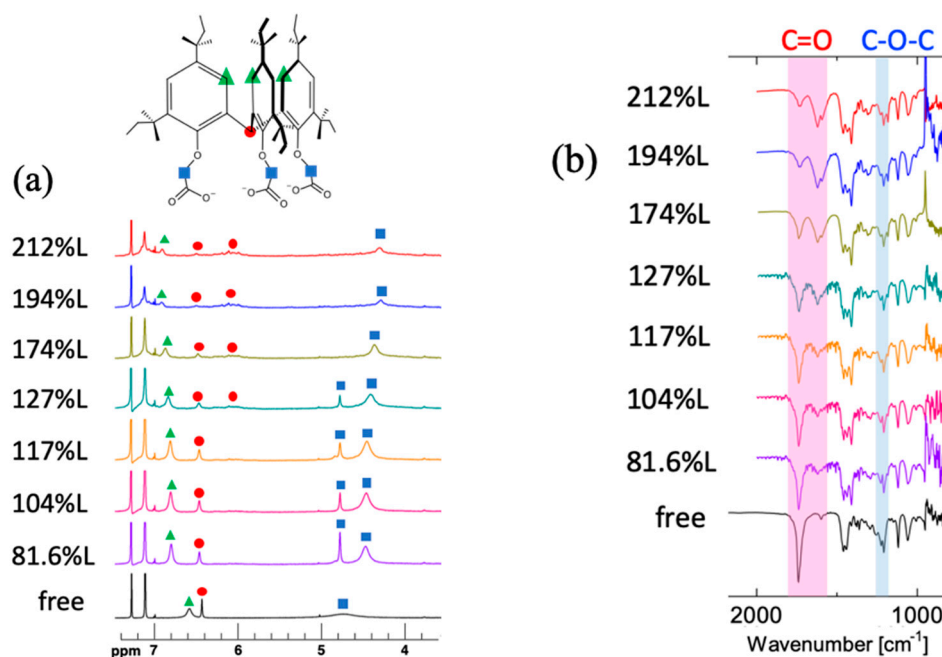


Figure 11. (a) $^1\text{H-NMR}$ and (b) IR spectra of free **3** and after loading with defined quantities of In^{3+} .

The resonances of free **1–3** in the $^1\text{H-NMR}$ spectra became sharper upon metal loading, presumably causing complex formation and reduced flexibility of the molecules. Moreover, only minor shifts were observed for the proton resonances of **1** after loading both Ga^{3+} and In^{3+} (Figures 6a and 7a). If the phenoxy oxygen atoms are involved in the complex formation, the molecular motion should be significantly suppressed. Accordingly, shifts representing the aryl protons (green triangles) would be expected, despite their distance from the coordination site, as structural changes in the cone conformational calix[4]arene caused by the metal uptake would lead to a change in the environment and a shielding of these protons [48–51]. Thus, only the carboxylates of **1** are involved in the coordination of Ga^{3+} and In^{3+} without structural changes in the calix[4]arene. This may be a result of a lack of consistency in the size of **1**, even with a larger In^{3+} . This observation supports the assumption that the coordination site of **1** is slightly larger than that of In^{3+} . Additional information was obtained from a detailed analysis of the IR spectra. After loading **1** with Ga^{3+} , the absorptions at approximately 1734 and 1396 cm^{-1} (attributed to carboxyl groups) were shifted to 1584 and 1409 cm^{-1} (Figure 6b), whereas the absorption at approximately 1202 cm^{-1} (attributed to aromatic ether groups) did not shift (Figure 6b). This may indicate that the coordination site of **1** is much larger than that of In^{3+} . Although the calix[4]arene derivative **1** accommodated a 200% In^{3+} loading, a notable peak shift was not observed (Figure 7a). However, a significant shift was observed from 1734 cm^{-1} to 1622 and 1583 cm^{-1} (Figure 7b). Remarkably, this shift appeared with over 100% loading. The unexpected stoichiometry of 1:2 (**1**: In^{3+}) is explained by “allosteric coextraction” [51–53], which likely occurred during the second metal extraction step with the surplus ion-exchangeable group, whose extraction ability was facilitated by the first metal extraction.

While the $^1\text{H-NMR}$ spectra of **2** revealed minor shifts in the proton resonances after loading with Ga^{3+} and In^{3+} (Figures 8a and 9a), a detailed elucidation of the involved donor atoms was not possible, although the metal coordination resulted in a detectable shift for the proton resonances adjacent to the donor atoms [54]. However, in the IR spectra, significant shifts from 1751 and 1726 , and 1182 cm^{-1} to 1734 , and 1220 cm^{-1} for Ga^{3+} loading were observed (Figure 8b), whereas significant shifts from 1751 and 1726 cm^{-1} to 1736 , and a significantly increased peak at 1182 cm^{-1} for the In^{3+} loading were observed (Figure 9b). These shifts indicate that both carboxylate and phenoxy oxygen atoms are involved in the coordination of the metal ions. Presumably, the donor atoms in **2** offer suitably sized

coordination sites for the coordination of both metal ions, which is reflected in their high extraction. One possible reason for this is the solubility of the metal complexes. The peaks of **2** decreased with an increase in loading. As listed in Table 1, the alkenyl trimethylol-type tripodal compounds exhibit a high hydrophilicity because they possess three polar groups with a single lipophilic nonenyl group, unlike the calix[4]arene derivative, which has four polar groups and four lipophilic groups. The high hydrophilicity of **2** may have caused the inconsistent pH dependency results for both Ga^{3+} and In^{3+} , as shown in Figure 4b. Thus, **2** should be applied differently, possibly as an adsorbent. Compared with that of **1** and **2**, a clear peak shift was evident in both the $^1\text{H-NMR}$ and IR spectra of **3** after loading with Ga^{3+} and In^{3+} (Figure 10a,b and Figure 11a,b). In contrast with that of **1**, the molecular motion in **3** was rapid and the 2-aryl peak did not split. There was also a drastic peak shift after metal-loading, while the peaks of the methylene protons split and the new peak increased with the metal loading. Notably, while the methine proton was not shifted by Ga-loading, it decreased and ultimately disappeared with In-loading. The IR spectra showed that the carbonyl peak absorption at 1738 cm^{-1} decreased for both metal loadings, and shifted to 1620 and 1589 cm^{-1} with In-loading. The ethereal peak at 1182 cm^{-1} also decreased with both metal loadings. Tripodal **3** also exhibited an unexpected stoichiometry of 1:2 ($\text{3}:\text{In}^{3+}$). This can be explained by “allosteric coextraction”, because while **3** provides only three acetic acid groups for neutralization of the In^{3+} charge, it also provides a very active triphenylmethyl proton for the second In^{3+} , which acts as carbon acid and has an estimated pK_a value of 30 [55–57]. While very weak, the acid has sufficient strength to form a metal complex [58]. If the triphenylmethyl anion serves as a cation exchanger, **3** with a methine proton, three phenoxy oxygen atoms, and three acetic acid groups located at the optimal position for metal chelation would generate allosteric extraction. When the indium concentration increased, the chelate effect from two acetic acid groups and a triphenylmethyl anion may be stronger than the converging effect of the three acetic acid groups, which would contribute to this coextraction, and consequently facilitate the allosteric coextraction. Notably, while the peak of this triphenylmethyl proton did not disappear after Ga^{3+} loading (Figure 10a), it disappeared after In^{3+} loading (Figure 11a). We propose using carbon acid as an extremely weak acid for allosteric coextraction in future research.

The proposed structures of Ga^{3+} and In^{3+} complexes with **1–3** are shown in Figure 12a–c.

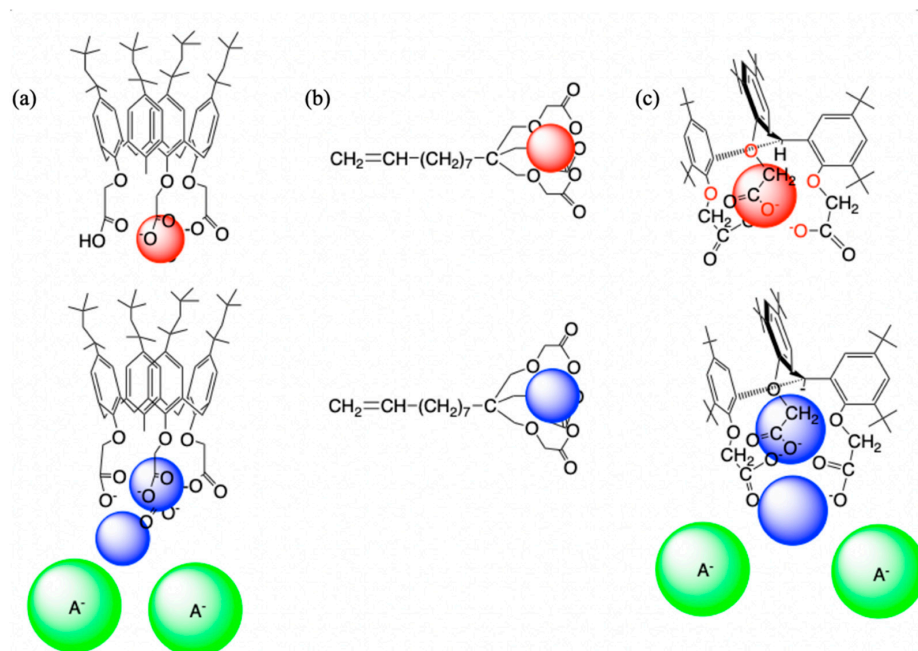


Figure 12. Proposed structures of Ga (red) and In (blue) complexes with (a) **1**, (b) **2**, and (c) **3**.

Three frameworks with different sized coordination sites and different extraction properties can be suitably designed for proper use.

4. Conclusions

Acetic acid derivatives of three different frameworks, calix[4]arene, alkenyltrimethylol, and tris(hydroxyphenyl)methane, with different numbers and sizes of their coordination sites, were prepared and the extraction of Al^{3+} , Ga^{3+} , and In^{3+} was investigated. They exhibited extremely high extraction capabilities compared with those of the corresponding monomeric and monopodal derivatives, owing to the convergence effects of the functional groups. The extraction reactions were determined using slope analysis, and the equilibrium extraction constants and $\text{pH}_{1/2}$ values for the aluminum group metal ions were determined. The extraction abilities, separation efficiencies, and coordination sites of the reagents were discussed using the obtained extraction data and the $^1\text{H-NMR}$ and IR spectroscopic data. For the extraction reagents with calix[4]arene and trihydroxytriphenylmethane frameworks, an unexpected stoichiometry of 1:2 (reagent: In^{3+}) was observed, which can be explained by allosteric coextraction. Based on the conclusions drawn in this study, extraction reagents can be tailored to selectively recover a target metal ion from a coexisting mixture of ions using suitable framework with coordination sites and donor atoms of particular sizes.

Supplementary Materials: The following are available online at <https://www.mdpi.com/article/10.3390/separations8110211/s1>, Figure S1: FT-IR spectra of 2.; Figure S2: $^1\text{H-NMR}$ spectra of 2.; Figure S3: $^{13}\text{C-NMR}$ spectra of 2.; Figure S4: FT-IR spectra of 5.; Figure S5: $^1\text{H-NMR}$ spectra of 5.; Figure S6: $^{13}\text{C-NMR}$ spectra of 5.; Figure S7: Effect of equilibrium pH on extraction percentage of Al (triangle), Ga (square), and In (circle) with carboxylic acid type of commercially available extraction reagent, neodecanoic acid (trade name Versatic acid 10, 150 mM in CHCl_3).

Author Contributions: Conceptualization, K.O.; validation, K.O., H.K. and S.M.; formal analysis, N.F. and H.F.; investigation N.F. and H.F.; data curation, K.O., M.W. and J.J.W.; writing—original draft preparation, K.O.; writing—review and editing, H.K., M.W. and J.J.W.; funding acquisition, K.O. and J.J.W. All authors have read and agreed to the published version of the manuscript.

Funding: This work was partially supported by the NEDO project “Research and Development of Recycling Technologies for Establishing a High Efficiency Resource Circulation System” and by a Japan Society for the Promotion of Science KAKENHI Grant-in-Aid for Scientific Research (C) [Grant number 19K12399]. We also thank the Erasmus+ program between TU Dresden and Saga University.

Institutional Review Board Statement: The study was conducted according to the guidelines of the Declaration of Helsinki, and approved by the Institutional Review Board of Saga University (Action of Educational staffs term 12 and January 2008).

Informed Consent Statement: Informed consent was obtained from all subjects involved in the study.

Data Availability Statement: Data are available from the authors upon the reasonable request.

Acknowledgments: The NMR measurements were conducted at the Analytical Research Center for Experimental Sciences, Saga University.

Conflicts of Interest: The authors declare no conflict of interest.

References

1. Pedersen, C.J. Cyclic polyethers and their complexes with metal salts. *J. Am. Chem. Soc.* **1967**, *89*, 2495–2496. [[CrossRef](#)]
2. Cram, D.J.; Cram, J.M. Host-guest chemistry. *Science* **1974**, *183*, 803–809. [[CrossRef](#)] [[PubMed](#)]
3. Pedersen, C.J. Cyclic polyethers and their complexes with metal salts. *J. Am. Chem. Soc.* **1967**, *89*, 7017–7036. [[CrossRef](#)]
4. Lehn, J.-M. Cryptates: Inclusion complexes of macropolycyclic receptor molecules. *Pure Appl. Chem.* **1978**, *50*, 871–892. [[CrossRef](#)]
5. Cram, D.J.; Kaneda, T.; Helgeson, R.C.; Lein, G.M. Spherands—ligands whose binding of cations relieves enforced electron-electron repulsions. *J. Am. Chem. Soc.* **1979**, *101*, 6752–6754. [[CrossRef](#)]
6. Cram, D.J.; Kaneda, T.; Lein, G.M.; Helgeson, R.C. A spherand containing an enforced cavity that selectively binds lithium and sodium ions. *J. Chem. Soc. Chem. Commun.* **1979**, 948b–950. [[CrossRef](#)]

7. Gutsche, C.D.; Muthukrishnan, R. Calixarenes. 1. Analysis of the product mixtures produced by the base-catalyzed condensation of formaldehyde with para-substituted phenols. *J. Org. Chem.* **1978**, *43*, 4905–4906. [[CrossRef](#)]
8. Yoshio, M.; Noguchi, H. Crown ethers for chemical analysis: A review. *Anal. Lett.* **1982**, *15*, 1197–1276. [[CrossRef](#)]
9. Vögtle, F.; Weber, E. (Eds.) *Host Guest Complex Chemistry III*; Topics in Current Chemistry Series; Springer: Berlin, Germany, 1984; Volume 121, pp. 1–104.
10. Izatt, R.M.; Pawlak, K.; Bradshaw, J.S.; Bruening, R.L. Thermodynamic and kinetic data for macrocycle interactions with cations and anions. *Chem. Rev.* **1991**, *91*, 1721–2085. [[CrossRef](#)]
11. Vögtle, F. Crown ethers, cryptands, podands and spherands. In *Supramolecular Chemistry: An Introduction*; John Wiley & Sons Ltd.: Chichester, UK, 1993; Chapter 2.2; pp. 27–83.
12. Cram, D.J.; Cram, J.M. Spherands, spheraplexes, and their relatives. In *Container Molecules and Their Guests, Monographs*; Stoddart, J.F., Ed.; RSC: Cambridge, UK, 1997; Chapter 2; pp. 20–48.
13. Arnaud-Neu, F.; Mckerverey, M.A.; Schwing-Weill, M.-J. Metal-ion complexation by narrow rim carbonyl derivatives. In *Calixarenes 2001*; Asfari, Z., Böhmer, V., Harrowfield, J.M., Vicens, J., Eds.; Kluwer Academic Publishers: Dordrecht, The Netherlands, 2001; Chapter 21, pp. 385–406.
14. Pedersen, C.J.; Frensdorff, H.K. Macrocyclic polyethers and their complexes. *Angew. Chem. Int. Ed.* **1972**, *11*, 16–25. [[CrossRef](#)]
15. Ohto, K. Research on various structural effects of calix[4]arene derivatives on extractive separation behavior of metal ions. *J. Ion Exch.* **2019**, *30*, 17–28. (In Japanese) [[CrossRef](#)]
16. Ohto, K.; Furugou, H.; Morisada, S.; Kawakita, H.; Isono, K.; Inoue, K. Stepwise recovery of molybdenum, tungsten, and vanadium by stripping using an amino-type “Trident” molecule by stripping. *Solvent Extr. Ion Exch.* **2021**, *39*, 512–532. [[CrossRef](#)]
17. Ohto, K. Review on adsorbents incorporating calixarene derivatives used for metals recovery and hazardous ions removal: The concept of adsorbent design and classification of adsorbents. *J. Incl. Phenom. Macrocycl. Chem.* **2021**, *101*, 175–194. [[CrossRef](#)]
18. Ohto, K. Molecular design and metal extraction behavior of calixarene compounds as host extractants. In *Ion Exchange and Solvent Extraction. Supramolecular Aspects of Solvent Extraction*; Moyer, B.A., Ed.; CPC Press: Boca Raton, FL, USA, 2013; Volume 21, Chapter 3, pp. 81–127.
19. Ohto, K.; Ueda, Y.; Sathuluri, R.R.; Kawakita, H.; Morisada, S.; Inoue, K. Silver extraction and recovery with macrocyclic and tripodal compounds. In *Silver Recovery from Assorted Spent Sources: Toxicology of Silver Ion*; Sabir, S., Ed.; World Scientific: New York, NY, USA, 2018; Chapter 9, pp. 275–301.
20. Yamaguma, R.; Yamashita, A.; Kawakita, H.; Miyajima, T.; Takemura, C.; Ohto, K.; Iwachido, N. Selective extraction of precious metal ions with novel trident molecules with pyridyl groups. *Sep. Sci. Technol.* **2012**, *47*, 1303–1309. [[CrossRef](#)]
21. Ohto, K.; Yamashita, A.; Ueda, Y.; Yamaguma, R.; Morisada, S.; Kawakita, H. Extractive removal of formaldehyde by using imination reaction with amine type of trident molecule. *Solvent Extr. Res. Dev. Jpn.* **2014**, *21*, 173–180. [[CrossRef](#)]
22. Ohto, K.; Furugou, H.; Yoshinaga, T.; Morisada, S.; Kawakita, H.; Inoue, K. Precious Metal Extraction with Thiol and Dithioether Derivatives of Trident Molecule. *Solvent Extr. Res. Dev. Jpn.* **2017**, *24*, 77–88. [[CrossRef](#)]
23. Ohto, K.; Fuchiwaki, N.; Yoshihara, T.; Chetry, A.B.; Morisada, S.; Kawakita, H. Extraction of scandium and other rare earth elements with a tricarboxylic acid derivative of tripodal pseudocalix[3]arene prepared from a new phenolic tripodal framework. *Sep. Purif. Technol.* **2019**, *226*, 259–266. [[CrossRef](#)]
24. Pearson, R.G. Hard and soft acids and bases. *J. Am. Chem. Soc.* **1963**, *85*, 3533–3539. [[CrossRef](#)]
25. Alfantazi, A.M.; Moskalyk, R.R. Processing of indium: A review. *Miner. Eng.* **2003**, *16*, 687–694. [[CrossRef](#)]
26. Zhan, L.; Xia, F.; Ye, Q.; Xiang, X.; Xie, B. Novel recycle technology for recovering rare metals (Ga, In) from waste light-emitting diodes. *J. Hazard. Mater.* **2015**, *299*, 388–394. [[CrossRef](#)]
27. Lu, F.; Xiao, T.; Lin, J.; Ning, Z.; Long, Q.; Xiao, L.; Huang, F.; Wang, W.; Xiao, Q.; Lan, X.; et al. Resources and extraction of gallium: A review. *Hydrometallurgy* **2017**, *174*, 105–115. [[CrossRef](#)]
28. Pradhan, D.; Panda, S.; Sukla, L.B. Recent advances in indium metallurgy: A review. *Miner. Process. Extr. Metall. Rev.* **2018**, *39*, 167–180. [[CrossRef](#)]
29. Sethurajan, M.; van Hullebusch, E.D.; Fontana, D.; Akcil, A.; Deveci, H.; Batinic, B.; Leal, J.P.; Gasche, T.A.; Kucuker, M.A.; Kuchta, K.; et al. Recent advances on hydrometallurgical recovery of critical and precious elements from end of life electronic wastes—A review. *Crit. Rev. Environ. Sci. Technol.* **2019**, *49*, 212–275. [[CrossRef](#)]
30. Zhao, Z.; Yang, Y.; Xiao, Y.; Fan, Y. Recovery of gallium from Bayer liquor: A review. *Hydrometallurgy* **2012**, *125*, 115–124. [[CrossRef](#)]
31. Nguyen, T.H.; Lee, M.S. A review on separation of gallium and indium from leach liquors by solvent extraction and ion exchange. *Miner. Process. Extr. Metall. Rev.* **2019**, *40*, 278–291. [[CrossRef](#)]
32. Nishihama, S.; Hino, A.; Hirai, T.; Komasa, I. Extraction and separation of gallium and indium from aqueous chloride solution using several organophosphorus compounds as extractants. *J. Chem. Eng. Jpn.* **1998**, *31*, 818–827. [[CrossRef](#)]
33. Hirayama, N.; Horita, Y.; Oshima, S.; Kubono, K.; Kokusen, H.; Honjo, T. Selective extraction of gallium from aluminum and indium using tripod phenolic ligands. *Talanta* **2001**, *53*, 857–862. [[CrossRef](#)]
34. Koshimoto, A.; Oshima, T.; Ohto, K.; Baba, Y. Synthesis of phosphonic acid extractants and selective extraction of In(III) and Ga(III) from acidic media containing Zn(II). *Solvent Extr. Res. Dev. Jpn.* **2011**, *18*, 137–147. [[CrossRef](#)]
35. Sasaki, Y.; Oshima, T.; Baba, Y. Mutual separation of indium(III), gallium(III) and zinc(II) with alkylated aminophosphonic acids with different basicities of amine moiety. *Sep. Purif. Technol.* **2017**, *173*, 37–43. [[CrossRef](#)]

36. Sasaki, Y.; Oshima, T.; Baba, Y. Synthesis of aminophosphonic acid extractants and the effect of the alkyl chain on their extraction selectivities for indium(III), gallium(III), and zinc(II). *Solvent Extr. Res. Dev. Jpn.* **2018**, *25*, 11–21. [[CrossRef](#)]
37. Sasaki, Y.; Uto, M.; Oshima, T.; Baba, Y. Synthesis of a carboxylic acid extractant containing an amino group and its selective extraction of In(III) and Ga(III). *Solvent Extr. Res. Dev. Jpn.* **2016**, *23*, 1–8. [[CrossRef](#)]
38. Sasaki, Y.; Matsuo, N.; Oshima, T.; Baba, Y. Selective extraction of In(III), Ga(III) and Zn(II) using a novel extractant with phenylphosphinic acid. *Chin. J. Chem. Eng.* **2016**, *24*, 232–236. [[CrossRef](#)]
39. Miura, R.; Tokumaru, M.; Oshima, T.; Baba, Y. Selective extraction of indium(III) and gallium(III) with 2-ethylhexyl thioglycolate. *Solvent Extr. Res. Dev. Jpn.* **2017**, *24*, 123–130. [[CrossRef](#)]
40. Adhikari, B.B.; Gurung, M.; Kawakita, H.; Ohto, K. Complexation and extraction behavior of trivalent indium with multiple proton ionizable p—t-butylcalix[5]arene pentacarboxylic acid derivative: A new efficient solvent extraction reagent for indium. *J. Incl. Phenom. Macrocycl. Chem.* **2011**, *71*, 479–487. [[CrossRef](#)]
41. Kawashima, M.; Kawakita, H.; Ohto, K.; Shiwa, Y. Aluminum group extraction with benzoic acid—Acetic acid crossed type calix[4]arene derivatives. *Solvent Extr. Res. Dev. Jpn.* **2012**, *19*, 41–50. [[CrossRef](#)]
42. Chetry, A.B.; Adhikari, B.B.; Morisada, S.; Kawakita, H.; Ohto, K. Selective extraction of Ga(III) with p-t-butylcalix[4]arene tetrahydroxamic acid. *Solvent Extr. Res. Dev. Jpn.* **2015**, *22*, 25–35. [[CrossRef](#)]
43. Pang, G.; Morisada, S.; Kawakita, H.; Hanamoto, T.; Umecky, T.; Ohto, K.; Song, X.-M. Allosteric extraction of a second gallium anion assisted by the first, loaded onto a fluorinated secondary amide reagent. *Sep. Purif. Technol.* **2021**, *278*, 119036. [[CrossRef](#)]
44. Ohto, K.; Yano, M.; Inoue, K.; Yamamoto, T.; Goto, M.; Nakashio, F.; Shinkai, S.; Nagasaki, T. Solvent extraction of trivalent rare earth metal ions with carboxylate derivatives of calixarenes. *Anal. Sci.* **1995**, *11*, 893–902. [[CrossRef](#)]
45. Ohto, K.; Nakagawa, H.; Furutsuka, H.; Shinohara, T.; Nakamura, T.; Oshima, T.; Inoue, K. Solvent extraction of rare earths with a novel phosphonate extractant providing a narrow coordination site. *Solvent Extr. Res. Dev. Jpn.* **2004**, *11*, 121–134.
46. Eigen, M. Fast elementary steps in chemical reaction mechanisms. *Pure Appl. Chem.* **1963**, *6*, 97–115. [[CrossRef](#)]
47. Ohto, K.; Ota, H.; Inoue, K. Solvent extraction of rare earths with a calix[4]arene compound containing phosphonate groups introduced onto upper rim. *Solvent Extr. Res. Dev. Jpn.* **1997**, *4*, 167–182.
48. Ohto, K.; Murakami, E.; Shinohara, T.; Shiratsuchi, K.; Inoue, K.; Iwasaki, M. Selective extraction of silver(I) over palladium(II) with ketonic derivatives of calixarenes from highly concentrated nitric acid. *Anal. Chim. Acta* **1997**, *341*, 275–283. [[CrossRef](#)]
49. Ohto, K.; Yamaga, H.; Murakami, E.; Inoue, K. Specific extraction behavior of amide derivative of calix[4]arene for silver(I) and gold(III) ions from highly acidic chloride media. *Talanta* **1997**, *44*, 1123–1130. [[CrossRef](#)]
50. Ohto, K.; Fujimoto, Y.; Inoue, K. Stepwise extraction of two lead ions with a single molecule of calix[4]arene tetracarboxylic Acid. *Anal. Chim. Acta* **1999**, *387*, 61–69. [[CrossRef](#)]
51. Ohto, K.; Ishibashi, H.; Kawakita, H.; Inoue, K.; Oshima, T. Allosteric coextraction of sodium and metal ions with calix[4]arene derivatives 1 Role of the first-extracted sodium ion as an allosteric trigger for self-coextraction of sodium ions with calix[4]arene tetracarboxylic acid. *J. Incl. Phenom. Macrocycl. Chem.* **2009**, *65*, 111–120. [[CrossRef](#)]
52. Yoneyama, T.; Sadamatsu, H.; Kuwata, S.; Kawakita, H.; Ohto, K. Allosteric coextraction of sodium and metal ions with calix[4]arene derivatives 2: First numerical evaluation for the allosteric effect on alkali metal extraction with crossed carboxylic acid type calix[4]arenes. *Talanta* **2012**, *88*, 121–128. [[CrossRef](#)]
53. Sadamatsu, H.; Morisada, S.; Kawakita, H.; Ohto, K. Allosteric coextraction of sodium and metal ions with calix[4]arene derivatives 3. Effect of propyl groups on size-discrimination for the second coextracted ion. *Solvent Extr. Ion Exch.* **2015**, *33*, 264–277. [[CrossRef](#)]
54. Ohto, K.; Yoshinaga, T.; Furugou, H.; Morisada, S.; Kawakita, H.; Inoue, K. Silver extraction with sulfide type trident compounds. *Solvent Extr. Res. Dev. Jpn.* **2018**, *25*, 71–78. [[CrossRef](#)]
55. Suzuki, S.; Kato, M.; Nakajima, S. Application of electrogenerated triphenylmethyl anion as a base for alkylation of arylacetic esters and arylacetonitriles and isomerization of allylbenzenes. *Can. J. Chem.* **1994**, *72*, 357–361. [[CrossRef](#)]
56. Bordwell, F.G. Equilibrium acidities in dimethyl sulfoxide solution. *Acc. Chem. Res.* **1988**, *21*, 456–463. [[CrossRef](#)]
57. Terrier, F.; Xie, H.-Q.; Lelievre, J.; Boubaker, T.; Farrell, P.G. Ionization of nitrotriphenylmethanes. Remarkable kinetic evidence for steric inhibition to resonance and F-strain. *J. Chem. Soc. Perkin Trans. 2* **1990**, *11*, 1899–1903. [[CrossRef](#)]
58. Olmstead, M.M.; Power, P.P. The isolation and x-ray structures of lithium crown ether salts of the free phenyl carbanions [CHPh₂]⁻ and [CPh₃]⁻. *J. Am. Chem. Soc.* **1985**, *107*, 2174–2175. [[CrossRef](#)]